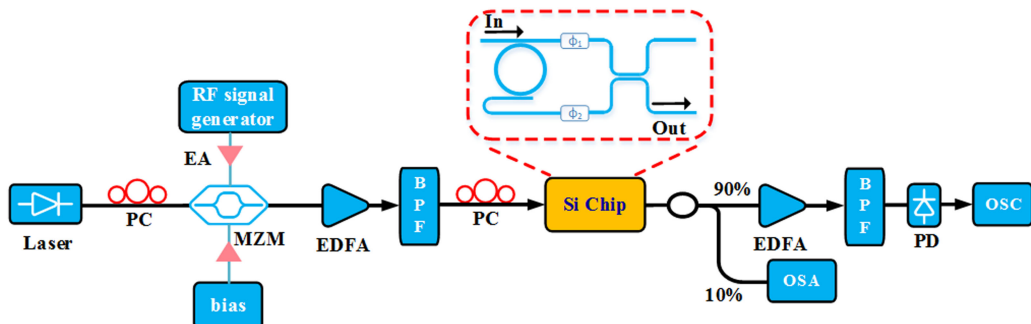


Tunable Silicon Photonic RF Phase Shifter With Low RF Power Variation Based on Constructive Interference of an Add-Drop Ring Resonator

Volume 10, Number 6, December 2018

Yanping Yu
Qihang Shang
Shaohua An
Yong Zhang
Yikai Su
Jianping Yao



DOI: 10.1109/JPHOT.2018.2884170
1943-0655 © 2018 IEEE

Tunable Silicon Photonic RF Phase Shifter With Low RF Power Variation Based on Constructive Interference of an Add-Drop Ring Resonator

Yanping Yu,¹ Qihang Shang,¹ Shaohua An,¹ Yong Zhang^{ID, 1}
Yikai Su^{ID, 1} and Jianping Yao^{ID, 2}

¹State Key Laboratory of Advanced Optical Communication Systems and Networks and the Department of Electronic Engineering, Shanghai Jiao Tong University, Shanghai 200240, China

²Microwave Photonics Research Laboratory, School of Electrical Engineering and Computer Science, University of Ottawa, Ottawa, ON K1N 6N5, Canada

DOI:10.1109/JPHOT.2018.2884170

1943-0655 © 2018 IEEE. Translations and content mining are permitted for academic research only.
Personal use is also permitted, but republication/redistribution requires IEEE permission.
See http://www.ieee.org/publications_standards/publications/rights/index.html for more information.

Manuscript received October 15, 2018; revised November 20, 2018; accepted November 26, 2018. Date of publication December 4, 2018; date of current version December 13, 2018. This work was supported in part by the National Natural Science Foundation of China under Grants 61835008 and 61860206001 and in part by the Science and Technology Commission of Shanghai Municipality under Grants 17500710900 and 16XD1401400. Corresponding author: Y. Su (e-mail: yikaisu@sjtu.edu.cn).

Abstract: We propose and experimentally demonstrate a tunable silicon photonic radio frequency (RF) phase shifter with low power variation based on constructive interference of an add-drop ring resonator. The thermal nonlinear effect of the add-drop ring resonator is used to realize a nearly 2π -phase shift, and the RF power variation is minimized by allowing two lights at the outputs of the add-drop ring resonator to combine at a directional coupler to achieve constructive interference. By thermally tuning the add-drop ring resonator, a nearly 2π -phase shift is realized and the operation is verified by an experiment. Experimental results show that a 0–5.2-rad phase-shift range with an RF power variation within 0.2 dB for a frequency range of a 40-GHz signal is achieved by thermally tuning the ring resonator. A phase shift up to 4.1 rad over a frequency range of 20–40 GHz is also realized.

Index Terms: Add-drop ring resonator, constructive interference, RF power variation, silicon photonic RF phase shifter.

1. Introduction

Phased-array antennas have been widely used in satellite communications [1] and radar systems [2]. Radio frequency (RF) phase shifters are key components in phased-array antennas. Electrical RF phase shifters usually have limited operation bandwidth and phase-shift range. Therefore, photonic RF phase with wider bandwidth and larger phase-shift range have been investigated [3]–[5]. Numerous schemes have been reported, such as the use of stimulated Brillouin scattering-induced slow light to achieve RF phase shift [6], the use of wavelength conversion in a distributed feedback (DFB) laser to produce a large phase change near the relaxation frequency, and to transfer the phase change to a RF signal [7], the use of a tilted fiber Bragg grating written in an Er/Yb co-doped fiber to generate slow-light-based RF phase shift [8], and the use of a slow light

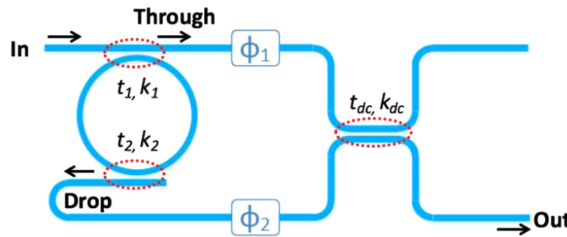


Fig. 1. Schematic diagram of the proposed device.

resulted from cascaded semiconductor optical amplifiers (SOAs) to produce a RF phase shift [9]. However, these approaches are all implemented based on discrete components, the size is large and the stability is poor. To reduce the size and to increase the stability, an effective solution is to use photonic integrated circuits (PICs).

PICs based on silicon-on-insulator (SOI) are attractive due to the compact footprint and complementary metal-oxide semiconductor (CMOS) compatible fabrication process. Recently, on-chip silicon microring resonators (MRRs) have been used to realize RF phase shifters [10]–[12]. For example, a broadband and tunable photonic RF phase shifter based on an MMR was demonstrated by us [10]. A phase shift range of 4.6 rad and a RF power variation of 3 dB at 40 GHz was experimentally demonstrated. The key limitation of the approach is its large RF power variation due to the deep notch of the silicon MRR, which will limit its practical applications [13]. A dual-microring resonator (DMRR) was used to realize a photonic RF phase shifter with smaller RF power variation [11]. It was demonstrated that a maximum 4.7-rad phase shift with a RF power variation of less than 2 dB was achieved. However, to achieve phase shift tuning, simultaneous adjustment of the resonance wavelengths of the two ring resonators is needed, which is a complicated process. In [12], by applying a bias voltage to a feedback-coupled ring resonator (FCMR), the RF power variation was reduced from 9 dB to 5 dB while a phase shift range of 3.0 rad was remained unchanged, but a 5-dB RF power variation is still high for practical applications.

In this paper, we propose and experimentally demonstrate a tunable silicon photonic RF phase shifter with small RF power variation based on constructive interference of an add-drop ring resonator. The thermal nonlinear effect of the add-drop ring resonator is used to realize a nearly 2π phase shift. The two lights at the outputs of the add-drop resonator are combined by a directional coupler. The constructive interference of the two lights is used to minimize the RF power variation. Simulation results show that a flat magnitude response of the proposed device can be obtained while the maximum phase shift is almost not affected by the constructive interference. Experimental results show that the photonic RF phase shifter can have a phase shift range of 0–5.2-rad with a power variation of less than 0.2 dB.

2. Principle

First, we discuss the operations of the proposed silicon photonic device which consists of an add-drop ring resonator and a directional coupler, as shown in Fig. 1. According to the scatter matrix [14], the electric fields at the output ports of the add-drop ring resonator can be expressed as

$$E_{through} = \frac{t_1 - t_2 a e^{j\phi}}{1 - t_1 t_2 a e^{j\phi}} E_{in}, \quad (1)$$

$$E_{drop} = \frac{-k_1 k_2 \sqrt{a e^{\frac{j\phi}{2}}}}{1 - t_1 t_2 a e^{j\phi}} E_{in}, \quad (2)$$

where $E_{through}$ and E_{drop} are the complex amplitudes of the signals from the through and drop ports of the ring resonator, respectively, t_i and k_i ($t_i^2 + k_i^2 = 1$, $i = 1, 2$) are the self-coupling and cross-coupling coefficients of the i th directional coupler, respectively, a is the round-trip amplitude

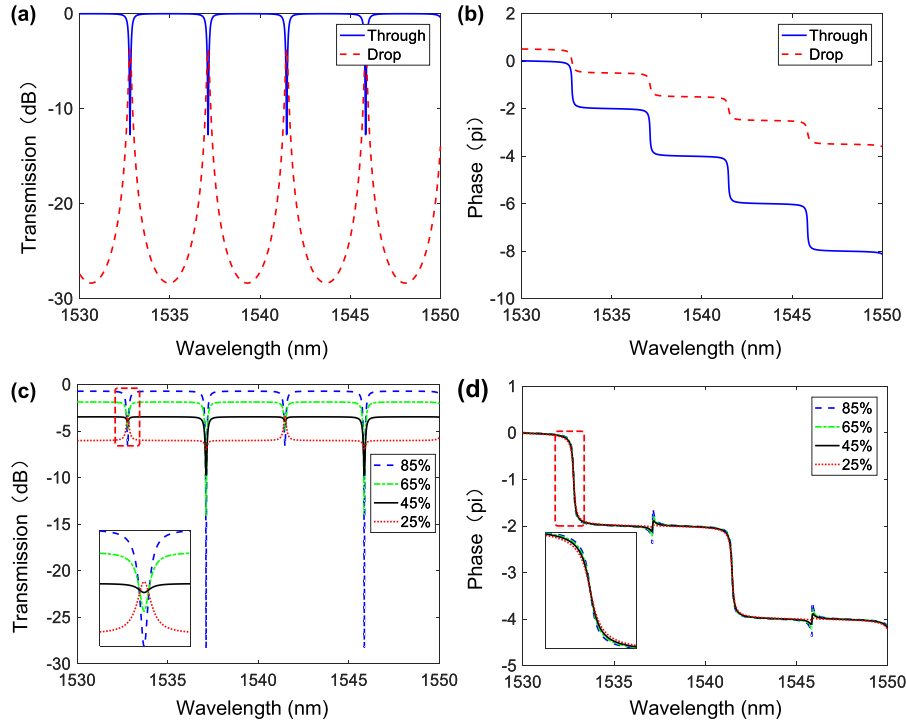


Fig. 2. (a) Transmission spectra at the through and drop ports. (b) Phase responses at the through and drop ports. (c) Transmission spectra at the output port with different t_{dc}^2 . (d) Phase responses at the output port with different t_{dc}^2 .

attenuation in the ring, and ϕ is the single-pass phase shift in the ring resonator, which is related with the wavelength of the input light. The parameters t_1 , t_2 and a are selected to satisfy the relationship given by $t_1 < t_2 a$, which means that the ring resonator works in the over-coupling condition.

The directional coupler combines the two output lights from the add-drop ring resonator and introduces a $\pi/2$ phase shift to the combined light [15]. To compensate for the coupling-induced phase shift, the phase difference $\phi_2 - \phi_1$ is set to be equal to $\pi/2$. Thus, the electric field at the output of the device can be written as

$$E_{out} = (t_{dc} E_{through} + k_{dc} E_{drop}) e^{j\phi_0}, \quad (3)$$

where t_{dc} and k_{dc} are the self-coupling and cross-coupling coefficients of the directional coupler, and ϕ_0 is the phase shift introduced to the two lights by controlling the phase difference to let $\phi_2 - \phi_1$ equal to $\pi/2$. Ignoring the fixed term $\exp(j\phi_0)$, the transmission function of the device can be expressed as

$$T = \frac{E_{out}}{E_{in}} = \frac{t_{dc}(t_1 - t_2 a e^{j\phi}) - k_{dc}(k_1 k_2 \sqrt{a} e^{j\phi/2})}{1 - t_1 t_2 a e^{j\phi}}. \quad (4)$$

Note that the original resonances of the add-drop ring resonator occur at $\phi = 2m\pi$ ($m = 1, 2, 3, \dots$). From Eq. (4), we can see that constructive interferences occur at resonance wavelengths if m is an even number while destructive interferences occur if m is an odd number. Thus the constructive and destructive interferences alternatively happen with the increase of m , due to the $e^{j\phi/2}$ term in Eq. (4). Fig. 2(a) and (b) shows the calculated transmission and phase responses of the add-drop ring resonator, respectively. The simulated magnitude and phase responses at the output of the device with different power splitting ratios t_{dc}^2 are shown in Fig. 2(c) and (d), respectively. The self-coupling coefficients of the directional couplers are $t_1 = 0.93$, $t_2 = 0.98$ and the radius of the ring resonator is $20 \mu\text{m}$. The linear loss factor α is 2 dB/cm and the group index n_g is 4.33 .

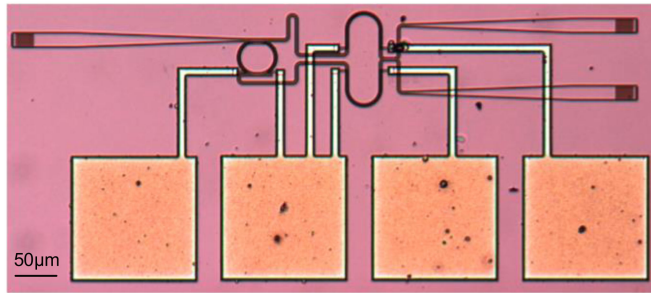


Fig. 3. Micrograph of the fabricated device.

By controlling the power splitting ratio t_{dc}^2 , half of the notches in transmission can be completely eliminated owing to the constructively interference shown in Fig. 2(c). From Fig. 2(d) we can see that the phase response remains almost unchanged with different power splitting ratios at the wavelengths where constructively interferences occur. Therefore, a maximum phase shift of nearly 2π is almost not affected by the constructive interference introduced by the directional coupler.

To use the device to achieve a photonic RF phase shifter, we generate two phase-correlated optical wavelengths with a frequency spacing of 40 GHz based on optical carrier-suppressed (OCS) modulation. The electric field of the phase-correlated optical wavelengths is expressed as

$$E_{in}(t) = A_- \exp[j(\omega_s - \omega_{RF})t] + A_+ \exp[j(\omega_s + \omega_{RF})t], \quad (5)$$

where A_- and A_+ represent the amplitudes of the two frequency components, ω_s and ω_{RF} are the frequencies of the optical carrier and the RF signal, respectively. Passing through the proposed device, the electric field of the OCS signal becomes:

$$E_{out}(t) = A_- T_- \exp[j(\omega_s - \omega_{RF})t] \exp(j\theta_-) + A_+ T_+ \exp[j(\omega_s + \omega_{RF})t] \exp(j\theta_+), \quad (6)$$

where T_\pm and $\exp(j\theta_\pm)$ are the transmission coefficients and the phase responses of the device at two sideband frequencies, respectively. A photodetector (PD) is used to detect the RF signal. The current at the output of the PD is given by

$$I_{PD} = 2R((A_- A_+)(T_- T_+) \cos[2\omega_{RF}t + (\theta_- - \theta_+)]), \quad (7)$$

where R is the responsivity of the PD.

By thermally tuning the add-drop ring resonator, the phase difference $\theta_- - \theta_+$ will change. It is different from a ring-resonator-based phase shifter [10], the proposed device has a flat magnitude response for a phase shift of nearly 2π . The transmission coefficients T_\pm remain almost unchanged owing to the flat magnitude response. Thus, tunable RF phase shift with low RF power variation is realized.

3. Fabrication, Experimental Setup, and Results

Fig. 3 shows the micrograph of the proposed device. The device was fabricated on a silicon-on-insulator platform. The cross section of the silicon waveguide is $500 \text{ nm} \times 220 \text{ nm}$. The thickness of the buried dioxide is $3 \mu\text{m}$. The radius of the add-drop microring resonator is $20 \mu\text{m}$. The desired self-coupling coefficients of t_1 , t_2 and t_{dc} are realized by setting proper coupling lengths and gaps of the directional couplers. For t_1 and t_2 , the coupling gaps are set to 240 nm and 330 nm, respectively. While for t_{dc} , the length and gap are set to $8 \mu\text{m}$ and 200 nm, respectively. E-beam lithography (EBL, Vistec EBPG 5200⁺) was used to define the device pattern. Then, the top silicon layer was etched by an inductively coupled plasma (ICP) etching process. A $1-\mu\text{m}$ -thick silica layer was deposited over the whole device as an upper cladding layer by plasma enhanced chemical vapor deposition (PECVD). Three 100-nm-thick Ti micro heaters and four $1-\mu\text{m}$ -thick Al pads were fabricated using

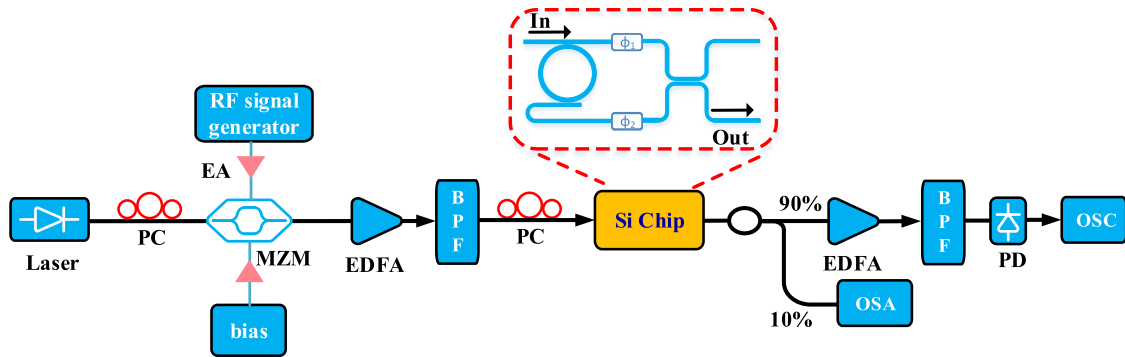


Fig. 4. Measurement setup for the proposed silicon photonic RF phase shifter.

lift-off processes. One of the heaters on the add-drop ring resonator tunes the RF phase shift, while the other two heaters on the silicon waveguides adjust the phase difference between the two output lights from the add-drop resonator.

Fig. 4 illustrates the measurement setup to evaluate the operation of the proposed photonic RF phase shifter. A continuous-wave optical carrier generated by a tunable laser source (Keysight 81960A) is sent to a Mach-Zehnder modulator (MZM) where it is modulated by a 20-GHz RF signal, generated by a RF signal generator (APSIN20G). An erbium-doped fiber amplifier (EDFA) is connected to the MZM to amplify the generated OCS signal, which is sent to the silicon chip via a single-mode fiber (SMF). To couple the OCS signal into and out of the silicon chip, two grating couplers are employed. The fiber-chip loss is measured which is about 7 dB per facet. Two polarization controllers (PCs) are used to adjust the polarization states of the optical wave to the MZM and to the device to minimize the polarization-dependent loss. At the output port of the silicon chip, a power splitter is used to divide the light into two parts, with one part being sent to an optical spectrum analyzer (OSA) to monitor the spectrum of the signal, and the other being amplified by a second EDFA and send to the PD via two tunable optical filters, to suppress the amplified spontaneous emission (ASE) noise from the EDFA. The recovered RF signal is recorded by an oscilloscope (OSC) and the phase shift and the RF power variation are evaluated by post processing.

In the experiment, we gradually increased the heating power applied on the waveguides and observed the transmission spectrum of the device. When the notch depth in the spectrum was minimized, the desired constructive interference between the two output lights from the add-drop ring resonator occurred. The transmission spectrum was measured as shown in Fig. 5. Half of the notches induced by the add-drop ring resonator have been eliminated, which is consistent with results obtained from the simulations. The resonance dips are not equal, due to the wavelength dependency of the directional couplers. As seen from Eq. (4), the transmission spectrum is dependent on the coupling ratios t_1 , t_2 and t_{dc} of the directional couplers. Thus small deviations of the coupling ratios lead to the different resonance dips at different resonance wavelengths in Fig. 5. The notch depth is about 0.5 dB at the resonance wavelength of 1552.40 nm, which is used to evaluate the phase shift of the RF signal. Obviously, the magnitude response of the device is flat enough to keep the power of the output RF signal with small variations during the tuning of the phase shift.

To realize a phase shift of the RF signal, the central wavelength of the OCS signal is set at 1552.73 nm on the right side of the resonance wavelength. Fig. 6(a) shows the spectrum of the OCS signal before it is injected into the device. By biasing the MZM to its transmission null, the optical carrier is suppressed. As the MZM is driven by a sinusoidal waveform, the output signal is with multiple side tones. An extinction ratio of 25 dB between the two central side tones and their neighboring frequency components is achieved, which ensures that a sinusoidal waveform with almost no harmonic distortion can be obtained. Note that there is a trade-off between the extinction

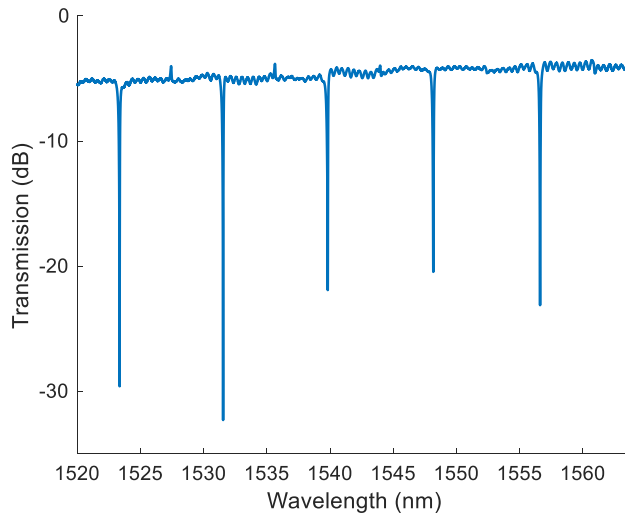


Fig. 5. Measured transmission spectrum of the fabricated device.

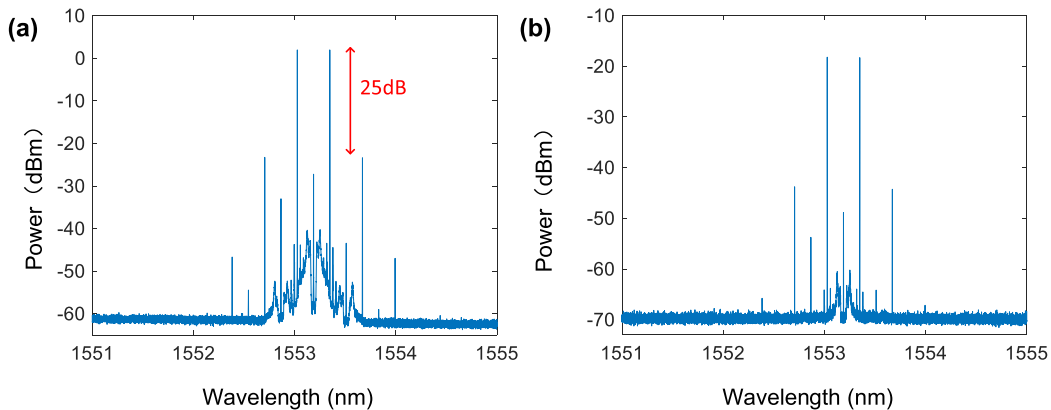


Fig. 6. Spectra of the OCS signal (a) at the input and (b) at the output of the device.

ratio and the available optical power of the OCS signal. The spectrum of the OCS signal at the output of the device is shown in Fig. 6(b). The power of the phase shifted RF signal is reduced by ~ 20 dB due to the fiber-chip coupling losses and the insertion loss of the device.

When a heating power is applied on the ring resonator, the waveform of the RF signal exhibits a time shift. We measured the time shifts with different heating powers and then converted them to the corresponding phase shifts. A maximum phase shift of 5.2 rad for the 40-GHz RF signal was obtained, as shown in Fig. 7(a). The intensity of the RF signal kept nearly constant during the phase-shifting operation. The power variation was less than 0.2 dB as shown in Fig. 7(b). And the RF gain was measured to be about -10 dB.

Fig. 8 depicts the phase shifts over a frequency range from 20 to 40 GHz with different tuning powers. To obtain the maximum phase shift, ~ 4.3 mW heating power was needed. The resonance bandwidth and the free spectral range (FSR) of the used ring resonator are about 0.40 nm and 4.2 nm, respectively. The frequency spacing of the OCS signal is smaller than the resonance bandwidth. Thus higher frequency of the RF signal is desired to fully utilize the phase-shift range in the phase-response spectrum of Fig. 2(d) [10]. A phase shift up to 4.1 rad over the bandwidth from 20 to 40 GHz can be obtained from Fig. 8. The phase-shift range decreases rapidly if the RF frequency is less than 20 GHz. Therefore, the lower limit of the RF frequency is mainly set by the

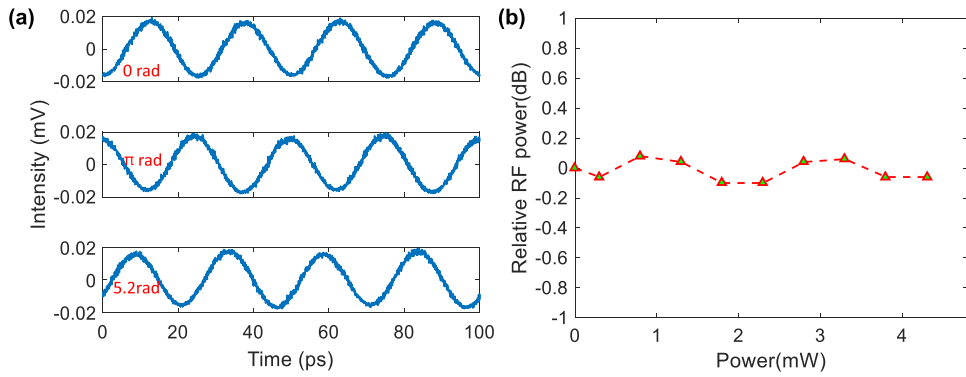


Fig. 7. (a) Waveforms of 40-GHz RF signal with different phase shifts. (b) Relative RF power versus the tuning power.

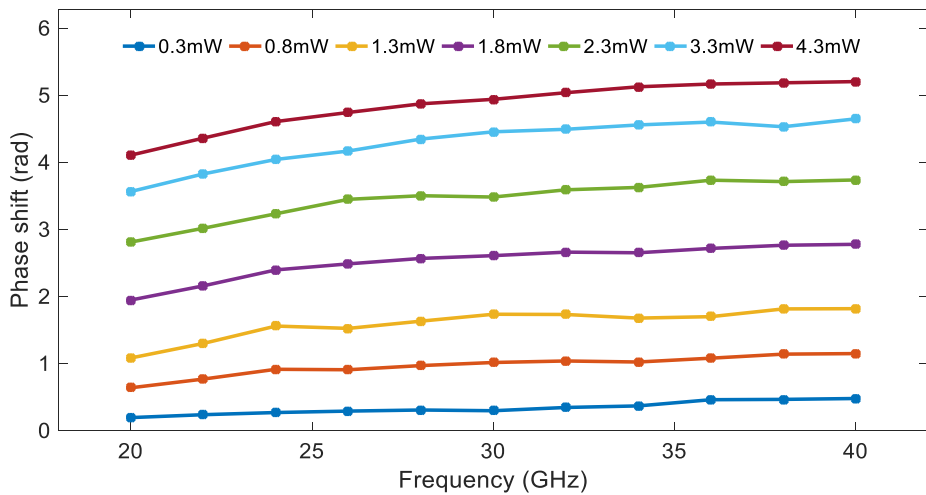


Fig. 8. Measured phase shifts over a frequency range from 20 to 40 GHz with different tuning powers.

resonance bandwidth of the resonator. Theoretically, the maximum RF frequency is only limited by the FSR of the used ring resonator, which is about 500 GHz. Thus the frequency range of the proposed RF photonic phase shifter is expected to be from 20 GHz to \sim 500 GHz. The response time is on the order of \sim 1 μ s [10].

4. Conclusion

In summary, we have proposed and experimentally demonstrated a silicon photonic RF phase shifter with low power variation based on constructive interference of an add-drop ring resonator. Simulation results showed that a flat magnitude response of the proposed device can be obtained owing to the constructive interference introduced by a directional coupler. The maximum phase shift of nearly 2π was almost not affected by the constructive interference. Experimental results showed a 0–5.2-rad phase-shift range with a RF power variation within 0.2 dB for a 40 GHz signal was achieved. In addition, a phase shift up to 4.1 rad over a frequency range from 20 to 40 GHz was realized. The frequency dependence of the proposed phase shifter is due to the wide resonance bandwidth. By employing a ring resonator with a narrower resonance bandwidth, the frequency dependency can be reduced.

Acknowledgment

The author would like to thank the Center for Advanced Electronic Materials and Devices of Shanghai Jiao Tong University for the support of device fabrication.

References

- [1] T. K. Wu, "Phased array antenna for tracking and communication with LEO satellites," in *Proc. Int. Symp. Phased Array Syst. Technol.*, 1996, pp. 293–296.
- [2] D. Gryglewski, T. Morawski, E. Sedek, and J. Zborowska, "Microwave phase shifters for radar applications," in *Proc. Int. Conf. Microw. Radar Wireless Commun.*, 2006, pp. 309–312.
- [3] J. F. Coward, C. H. Chalfant, and P. H. Chang, "A photonic integrated-optic RF phase shifter for phased array antenna beam-forming applications," *J. Lightw. Technol.*, vol. 11, no. 12, pp. 2201–2205, Dec. 1993.
- [4] A. J. Seeds and K. J. Williams, "Microwave photonics," *J. Lightw. Technol.*, vol. 24, no. 12, pp. 4628–4641, Dec. 2006.
- [5] J. Capmany, J. Mora, I. Gasulla, J. Sancho, J. Lloret, and S. Sales, "Microwave photonic signal processing," *J. Lightw. Technol.*, vol. 31, no. 4, pp. 571–586, Feb. 2013.
- [6] J. Sancho *et al.*, "Dynamic microwave photonic filter using separate carrier tuning based on stimulated brillouin scattering in fibers," *IEEE Photon. Technol. Lett.*, vol. 22, no. 23, pp. 1753–1755, Dec. 2010.
- [7] M. R. Fisher and S. L. Chuang, "A microwave photonic phase-shifter based on wavelength conversion in a DFB laser," *IEEE Photon. Technol. Lett.*, vol. 18, no. 16, pp. 1714–1716, Aug. 2006.
- [8] H. Shahoei and J. Yao, "Tunable microwave photonic phase shifter based on slow and fast light effects in a tilted fiber Bragg grating," *Opt. Express*, vol. 20, no. 13, pp. 14009–14014, Jun. 2012.
- [9] W. Xue, S. Sales, J. Capmany, and J. Mørk, "Microwave phase shifter with controllable power response based on slow- and fast-light effects in semiconductor optical amplifiers," *Opt. Lett.*, vol. 34, no. 7, pp. 929–931, Apr. 2009.
- [10] Q. Chang, Q. Li, Z. Zhang, M. Qiu, T. Ye, and Y. Su, "A tunable broadband photonic RF phase shifter based on a silicon microring resonator," *IEEE Photon. Technol. Lett.*, vol. 21, no. 1, pp. 60–62, Jan. 2009.
- [11] M. Pu *et al.*, "Widely tunable microwave phase shifter based on silicon-on-insulator dual-microring resonator," *Opt. Exp.*, vol. 18, no. 6, pp. 6172–6182, Mar. 2010.
- [12] J. Tang, M. Li, S. Sun, Z. Li, W. Li, and N. Zhu, "Broadband microwave photonic phase shifter based on a feedback-coupled microring resonator with small radio frequency power variations," *Opt. Lett.*, vol. 41, no. 20, pp. 4609–4612, Oct. 2016.
- [13] M. Pu *et al.*, "Tunable microwave phase shifter based on silicon-on-insulator microring resonator," *IEEE Photon. Technol. Lett.*, vol. 22, no. 12, pp. 869–871, Jun. 2010.
- [14] A. Yariv, "Critical coupling and its control in optical waveguide-ring resonator systems," *IEEE Photon. Technol. Lett.*, vol. 14, no. 4, pp. 483–485, Apr. 2002.
- [15] S. Darmawan, L. Y. M. Tobing, and T. Mei, "Coupling-induced phase shift in a microring-coupled Mach–Zehnder interferometer," *Opt. Lett.*, vol. 35, no. 2, pp. 238–240, Jan. 2010.